

Article

Online Determination of Boron Isotope Ratio in Boron Trifluoride by Infrared Spectroscopy

Weijiang Zhang, Yin Tang and Jiao Xu *

School of Chemical Engineering & Technology, Tianjin University, Tianjin 300072, China; wjzh@tju.edu.cn (W.Z.); tangyin0001@163.com (Y.T.)

* Correspondence: xujiaohh@163.com; Tel.: +86-022-27402028

Received: 17 September 2018; Accepted: 3 December 2018; Published: 6 December 2018



Abstract: Enriched boron-10 and its related compounds have great application prospects, especially in the nuclear industry. The chemical exchange rectification method is one of the most important ways to separate the ^{10}B and ^{11}B isotope. However, a real-time monitoring method is needed because this separation process is difficult to characterize. Infrared spectroscopy was applied in the separation device to realize the online determination of the boron isotope ratio in boron trifluoride (BF_3). The possibility of determining the isotope ratio via the $2\nu_3$ band was explored. A correction factor was introduced to eliminate the difference between the ratio of peak areas and the true value of the boron isotope ratio. It was experimentally found that the influences of pressure and temperature could be ignored. The results showed that the infrared method has enough precision and stability for real-time, in situ determination of the boron isotope ratio. The instability point of the isotope ratio can be detected with the assistance of the online determination method and provides a reference for the production of boron isotope.

Keywords: isotope; boron; infrared spectroscopy; online determination

1. Introduction

Boron in naturally occurring compounds is composed of two isotopes, one of mass 10 and the other of mass 11. ^{10}B at a relative abundance of 18.8%, has an unusually large cross section for the capture of low energy neutrons [1]. Therefore, in high concentrations, it is particularly valuable for neutron shielding [2,3].

The design and realization of the isotopes separation processes of boron began as early as the Second World War. A large industrial plant with a productivity of up to 300 kg per year of elemental boron with 95% ^{10}B content was put into operation in 1944 [4]. At present, the most common methods for the separation of boron isotopes include the distillation method [5], chemical exchange rectification [6,7], ion exchange [8,9], and laser isotope separation [10,11], among others. Chemical exchange rectification is the simplest and most productive method for the separation of ^{10}B and ^{11}B isotopes at concentrations of 95% and over [12]. Figure 1 shows the principal scheme of the apparatus for the separation of boron isotopes using the chemical exchange rectification method. ^{10}B and ^{11}B can be extracted from the separation and the complex parts of the apparatus, respectively [13]. The internal variations in this separation process tend to be very complex, making it necessary to frequently track any changes in the isotope ratio obtained.

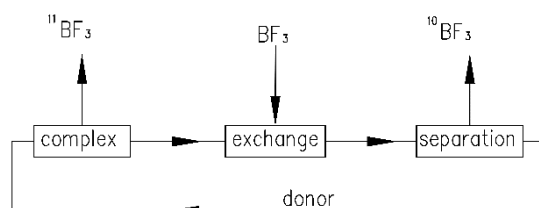


Figure 1. Principal scheme of the apparatus for the separation of boron isotopes using the chemical exchange rectification method.

The mass spectrometry (MS) method is one of the most important ways of analyzing the boron isotope ratio. Analysis comes from the peaks with mass-to-charge ratios (m/e^+) equal to 10 and 11 [14]. Porteous [15] et al. determined the isotopic ratio of boron in samples of groundwater by inductively coupled plasma mass spectrometry (ICP-MS) to evaluate possible levels of boron pollution from anthropogenic inputs into natural aqueous systems. The matrix effect was reduced by the preconcentration and ion-exchange of the sample. Compared with the standard material, the precision of the method achieved 0.13% (natural abundance). However, the sampling and preparation for this method are very complex, so it is difficult to achieve real-time tracking for this process during actual production. Infrared spectroscopy (IR) is a traditional technology that has been used for on-line detection. For instance, Hepburn [16] et al. established a method using online FTIR spectroscopy to determine the siloxane content in bio-gas. Both the precision and the detection limit for siloxane were satisfactory when using this online FTIR technology.

The vibrational spectra of BF_3 has been studied by Herrebout [17,18] et al. and Sluyts [19] et al. The results were obtained by dissolving BF_3 in liquid Argon. The infrared absorption bands changed depending on the change in the boron isotope ratio. Thus, the bands could be used to measure the boron isotopic ratio in BF_3 . Despite having a good signal-noise ratio in the ν_3 region, such a high dilution factor was difficult to realize via changing optical paths in the industrialized process. Although the $2\nu_3$ is a weak IR absorption band for BF_3 , the difference in absorbance peaks was about 112 cm^{-1} between $^{10}\text{BF}_3$ and $^{11}\text{BF}_3$ at the $2\nu_3$ bands, which means that there is good resolution for this measurement. In this paper, the IR method was applied to determine the boron isotope ratio based on calculating the BF_3 infrared spectrum at $2\nu_3$. Further, an infrared spectrophotometer was installed in a boron separation device to monitor the separation process online.

2. Experimental Method

2.1. Instruments and Reagents

The BF_3 was purchased from LiuFang Gas Corporation (Dalian, LN, China) with a stated purity of 99.95%. Small amounts of SiF_4 were present as an impurity in the BF_3 but these were ignored in this study. NIST SRM 951a isotopic reference material of boric acid ($^{10}\text{B}/^{11}\text{B}$ is 0.2473 ± 0.0002) was purchased from the National Institute of Standards and Technology (Gaithersburg, MD, USA). A gas cell (TianGuang Optical Instrument Co. Ltd., Tianjin, TJ, China) was equipped with the CaF_2 windows ($\varnothing 40 \times 5\text{ mm}$). The optical path length of this gas cell was 100 mm. An infrared spectrophotometer (Xintian Optical Analytical Instrument Co. Ltd., Tianjin, TJ, China) with an accuracy of transmittance lower than or equal to $\pm 0.2\%$ T. (TJ270-30A, Tianjin, China). The $^{10}\text{B}/^{11}\text{B}$ ratio was measured as a reference by an ICP-MS X7 (Thermo Electron Corporation, Waltham, MA, USA) series mass spectrometer manufactured by the Thermo Electron Corporation.

2.2. Procedure for Offline Measurement

The procedure for the offline experiment is shown in Figure 2. BF_3 gas samples with different amounts of boron were collected from the chemical exchange rectification device or feed gas cylinder. The outlet of the gas cell was linked to a buffer bottle and an absorber bottle filled with sodium

hydroxide solution to prevent BF_3 gas from escaping. BF_3 was filling into the gas cell, which was replaced by N_2 to remove the air (especially the water in air) inside of the gas cell beforehand. This was allowed to continue for at least 1–2 min, and the operation was stopped when the inside of the gas cell was fully replaced by BF_3 . The valves of the gas cylinder and gas cell were closed in turn for about 10 min before use. The infrared spectra were acquired from scanning the contents of the gas cell at a scanning speed of $1 \text{ cm}^{-1}/\text{s}$ and a scanning range of 4000 to 400 cm^{-1} .

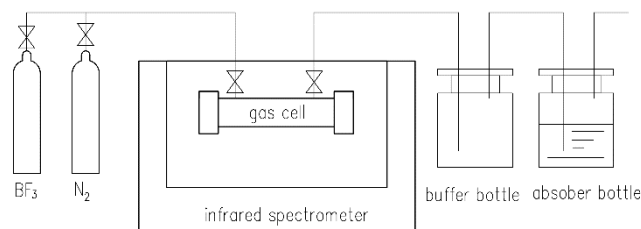


Figure 2. Diagram of offline experiment.

2.3. Procedure for Online Measurement

The online isotopic ratio determination system was set on the device used for boron isotope separation, as shown in Figure 3. The BF_3 gas was extracted from a pipe where the gas flow and the pipeline can be controlled by valve. The BF_3 flowed through a gas cell that was equipped with two CaF_2 windows because the weatherability and corrosion resistance of CaF_2 are superior to KBr under atmospheric and BF_3 conditions. The whole gas cell was fitted to the IR spectrophotometer by which the infrared spectrogram could be obtained directly.

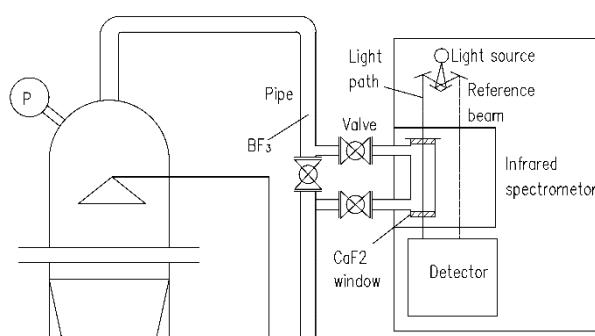


Figure 3. Diagram of boron isotope ratio online determination system.

2.4. Testing method of ICP-MS

The ICP-MS was used to determine the isotope ratio as a reference. The BF_3 gas was absorbed by a small amount of ethanol and diluted to samples containing $0.1 \mu\text{g}/\text{mL}$ of boron with ultrapure water. The operation method and experimental conditions of the ICP-MS experiments were similar to the method found in [15]. After each test, the system pipeline was alternately washed three times with 2% HNO_3 and 0.1 mol/L ammonia water solution to reduce any errors due to memory effect. The specific parameters used for the ICP-MS experiments to determine the boron isotope ratios ($^{10}\text{B}/^{11}\text{B}$) are shown in Table 1.

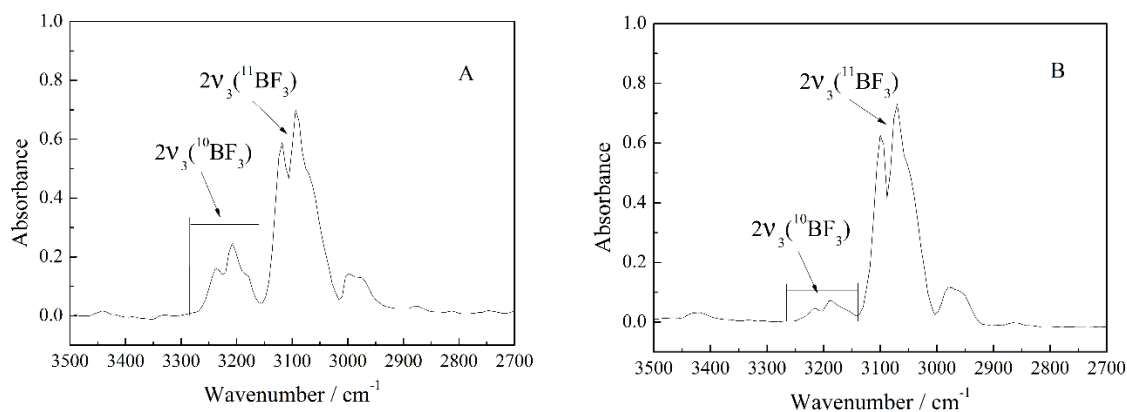
Table 1. Experimental conditions and parameters of inductively coupled plasma mass spectrometry (ICP-MS). Counts per Second (CPS); Atomic Mass Unit (AMU).

Item	Parameter	Item	Parameter
Nebulizer	Microconcentric Nebulizer	Sensitivity/s ⁻¹ (μg·L ⁻¹) ⁻¹	1.759 × 10 ⁶ CPS
Spray chamber temperature/°C	3	Scanning mode	Peak-jump
Nebulizer gas flow/L·min ⁻¹	0.93	Dwell time/ms	10
Auxiliary gas flow/L·min ⁻¹	0.9	Acquisition degree	10
Cool gas flow/L·min ⁻¹	10	Acquisition time/s	20
Plasma power/W	1250	Channels per AMU	3
Resolution	Standard	Runs/replicates	3
Sample uptake rate/mL·min ⁻¹	1	Sample depth/mm	104
Ionization lens parameters	L1 3.8; L2 31.8; L3 189.8	-	-

3. Results and Discussion

3.1. Calculation and Correction of the Isotope Ratio

Figure 4 shows the comparison of the IR spectrograms in the $2\nu_3$ regions between natural abundance BF_3 and enriched $^{11}\text{BF}_3$. The peaks at these regions are more complex than peaks in the ν_3 regions. Fortunately, the peak changes had no significant overlap of the two bands. By contrast, the absorption band of $2\nu_3$ for $^{10}\text{BF}_3$ (the range being about 3270–3170 cm^{-1}) was significantly reduced, which proved that this absorption band is influenced by the amount of $^{10}\text{BF}_3$ that is present. In contrast, the absorption peaks in the $2\nu_3$ band for $^{11}\text{BF}_3$ (the range being about 3170–3070 cm^{-1}) varied regularly with changing concentrations of $^{11}\text{BF}_3$. Thus, it was feasible to calculate the isotope ratio based on comparing the peak areas of these two absorption bands.

**Figure 4.** Comparison of the IR spectrograms. (A) Natural abundance BF_3 ; (B) Enriched $^{11}\text{BF}_3$.

The NIST SRM 951a boric acid standard sample was used to investigate the accuracy of the ICP-MS. Before testing by ICP-MS, the standard boric acid sample was dissolved and diluted to a solution containing 0.1 $\mu\text{g}/\text{mL}$ of boron with ultrapure water. The relative error between the result from the ICP-MS and the standard value is shown in Table 2.

Table 2. Accuracy experiment of ICP-MS.

$^{10}\text{B}/^{11}\text{B}$ Results of ICP-MS						Mean Value	$^{10}\text{B}/^{11}\text{B}$ Value of Standard Material	Relative Error/%
1	2	3	4	5	6			
0.2471	0.2464	0.2469	0.2468	0.2469	0.2475	0.2469	0.2473 ± 0.0002	0.16

The relative error between the experimental result from the ICP-MS and the isotopic ratio of the standard material was less than 0.16%. This result indicated that the ICP-MS, which was used to determine the boron isotope ratio in solution has a high accuracy, and could be used to calibrate the isotope ratio of boron in BF_3 . In Figure 4, the isotopic ratio values of the samples were calibrated by ICP-MS. The $^{10}\text{B}/^{11}\text{B}$ ratios of the natural abundance BF_3 and enriched $^{11}\text{BF}_3$ samples were 0.2473 ± 0.0009 and 0.0526 ± 0.0011 , respectively.

$^{10}\text{BF}_3$ and $^{11}\text{BF}_3$ could be regarded as two distinct forms of matter. As is shown in Figure 5, the graph shape of A_{10} represents peaks of $2\nu_3$ of $^{10}\text{BF}_3$. Similarly, A_{11} represents $2\nu_3$ peaks for $^{10}\text{BF}_3$. The baselines of the spectrograms were adjusted to zero before calculation. The experiments were processed at room temperature (25 ± 3 °C).

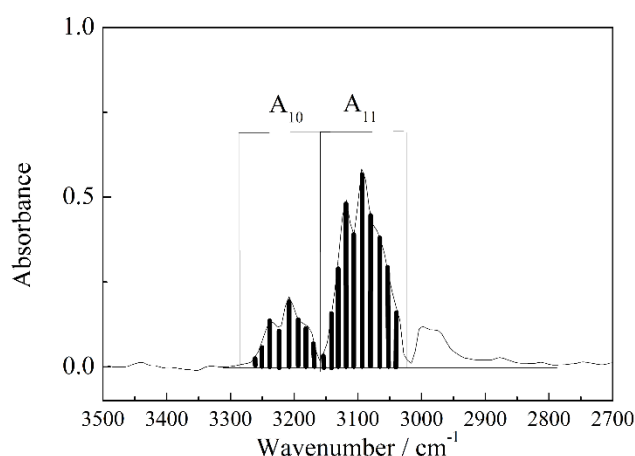


Figure 5. Schematic of the calculation method.

It is obvious that the difference in the peak integration value is significant between the A_{10}/A_{11} and the true value of $^{10}\text{B}/^{11}\text{B}$, and this is most likely due to $^{10}\text{BF}_3$ and $^{11}\text{BF}_3$ having different molar absorption coefficients at the $2\nu_3$ band. According to Lambert-Beer theory:

$$\lg(I_0/I) = \varepsilon \times b \times c \quad (1)$$

where, ε is the molar absorption coefficient, c is the molarity of the substance (mol/L), b is the optical length (cm), and $\lg(I_0/I)$ is the absorbance at the specific wavenumber. A_{10} or A_{11} could be regarded as the addition of several fixed number of absorptions roughly:

$$\begin{aligned} A_{10}/A_{11} &= \frac{\sum_{i=1}^n \lg(I_0/I_{10})_i}{\sum_{i=1}^n \lg(I_0/I_{11})_i} \\ &= \frac{\sum_{i=1}^n \varepsilon_{10i} b_{10i} c_{10i}}{\sum_{i=1}^n \varepsilon_{11i} b_{11i} c_{11i}} \end{aligned} \quad (2)$$

For $b_{10} = b_{11}$, c_{10i}/c_{11i} is a constant for the same gas (fixed concentration). Then:

$$A_{10}/A_{11} = \left(\frac{\sum_{i=1}^n \varepsilon_{10i}}{\sum_{i=1}^n \varepsilon_{11i}} \right) \times (c_{10}/c_{11}) \quad (3)$$

Let $\frac{\sum_{i=1}^n \varepsilon_{10i}}{\sum_{i=1}^n \varepsilon_{11i}} = K$. K , which is the correction factor, then:

$$K = A_{11}/A_{10} \times c_{10}/c_{11} \quad (4)$$

and

$$c_{10}/c_{11} = A_{11}/A_{10} \times K \quad (5)$$

The correction factor, K , is the ratio of the addition of a series of molar absorption coefficients in essence according to Equations (1)–(5). So, boron isotope ratio can be calculated by the peak areas of A_{10} and A_{11} . The correction factor can be obtained by testing the BF_3 gas of a known isotope ratio. Table 3 shows the continuous determination results of the A_{10}/A_{11} ratio for the normal, natural abundance BF_3 sample. The ICP-MS result of $^{10}\text{B}/^{11}\text{B}$ for this sample is 0.2473. While, the isotope ratio of $^{10}\text{B}/^{11}\text{B}$ is equal to c_{10}/c_{11} , based on the ICP-MS result and Equation (5), the value of correction factor K is 0.5431.

Table 3. Investigation of the correction factor by continuous determination of the ratio of A_{10}/A_{11} of the natural abundance BF_3 .

A_{10}/A_{11} (by IR Method)			Mean Value	RSD/%	$^{10}\text{B}/^{11}\text{B}$ (by ICP-MS ¹)	K
0.4508	0.4513	0.4634	0.4553	1.16	0.2473 ± 0.0009	0.5431
0.4585	0.4601	0.4512				
0.4535	0.4498	0.4515				
0.4626						

¹ mean and standard deviation were obtained from 3 determinations.

3.2. Precision Experiment for the IR Method

The precision experiment was achieved by continuous measurements of a group of samples of a known isotope ratio, and the results are shown in Table 4. The relative standard deviation (RSD) was calculated by Equation (6),

$$RSD = \frac{S}{\bar{x}} \times 100\% = \frac{\sqrt{\frac{\sum_{i=1}^n (x_i - \bar{x})^2}{n-1}}}{\bar{x}} \times 100\% \quad (6)$$

where, S is the standard deviation, \bar{x} is the mean value of the results of n tests, and n is the number of tests. The RSD of the samples with the higher levels of isotope ratio were less than 2.00%. Although the RSD of the sample where the $^{10}\text{B}/^{11}\text{B}$ ratio was 0.0506 (by ICP-MS) was more than 5.00%, the mean value of the IR method was close to the results from the ICP-MS experiments. These results indicated that the IR method is more precise when determining the boron isotope ratio.

Table 4. Precision experiment for the IR method.

$^{10}\text{B}/^{11}\text{B}$ (by ICP-MS)	Sample ($^{10}\text{B}/^{11}\text{B}$, by IR Method)						Mean Value	S	RSD/%
	1	2	3	4	5	6			
1.2351	1.2290	1.2382	1.2401	1.2320	1.2355	1.2413	1.2360	0.0048	0.39
0.2473	0.2405	0.2428	0.2451	0.2422	0.2506	0.2472	0.2447	0.0037	1.52
0.0506	0.0559	0.0532	0.0485	0.0511	0.0463	0.0509	0.0510	0.0034	6.64

3.3. Influence of the Pressure and Temperature

Due to the effect of the concentration of BF_3 , absorbance values grew with an increase in pressure. In addition, an increase in the temperature made the peak pattern wilder. Figure 6A,B show the influence of pressure and temperature on the isotope ratio of $^{10}\text{B}/^{11}\text{B}$, with the ranges of pressure and temperature being the possible interval values for the chemical exchange rectification operation. It was found that both the pressure and temperature have little impact on the isotope ratio determination results. Nevertheless, the optimum operation temperature was in the range of 278 to 298 K, because the errors might increase significantly when the temperature is higher than 303 K.

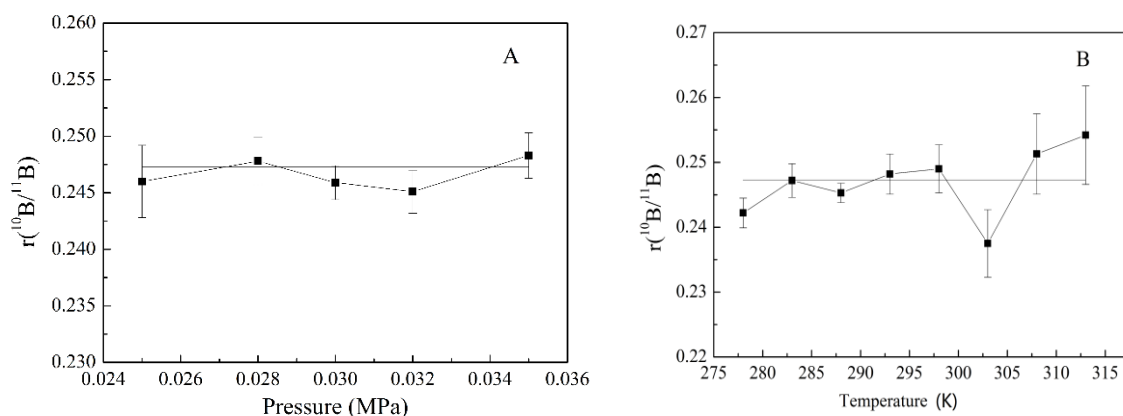


Figure 6. Influence of pressure and temperature on the isotope ratio of $^{10}\text{B}/^{11}\text{B}$. (A) Influence of pressure; (B) Influence of temperature.

3.4. Investigation of the Enriched BF_3 Gas by IR

Figure 7 shows the IR spectrograms for an enriched $^{10}\text{BF}_3$ sample and an enriched $^{11}\text{BF}_3$ sample. It is clearly observed in Figure 7A that when the concentration of ^{10}B decreased, the absorption peaks of A_{10} were reduced and the A_{11} peaks increased. Similarly, the absorption peaks of A_{11} were reduced and the A_{10} peaks were increased in Figure 7B. The calculation results for the samples in Figure 7A,B were 0.0120 and 0.7536, respectively. All of the results were in good agreement with the ICP-MS as a reference standard (the isotope ratios for Figure 7A,B were 0.0102 and 0.7546, respectively) for each sample, which proved the validity of the IR method. A series of enriched BF_3 samples, with their isotopic ratios determined by IR, are listed in Table 5, with the mean and standard deviation obtained from 10 determinations. By comparing the results of the IR method and the ICP-MS method, the errors of measurement increased slightly when determining the ratio of high abundance samples. This could be attributed to the decline in the signal-noise ratio (SNR), which was caused by the decrease in the absorbance value.

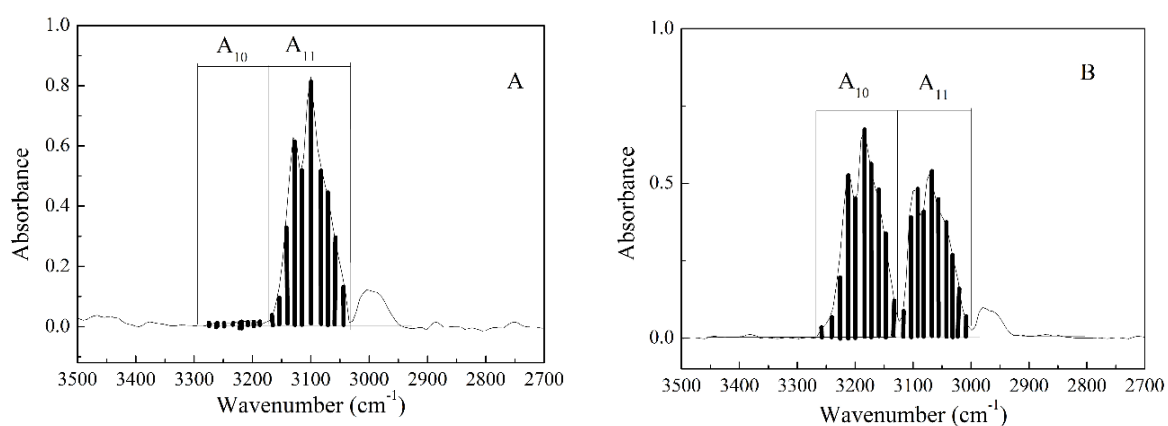


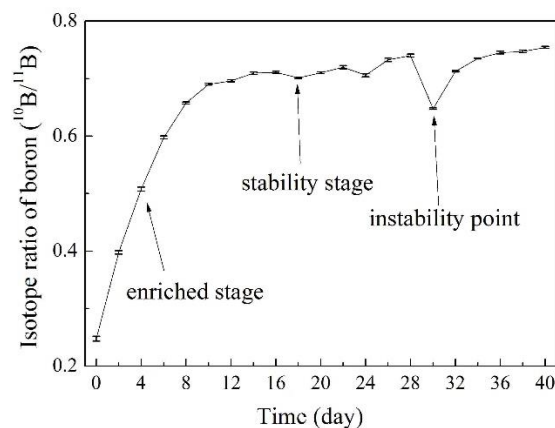
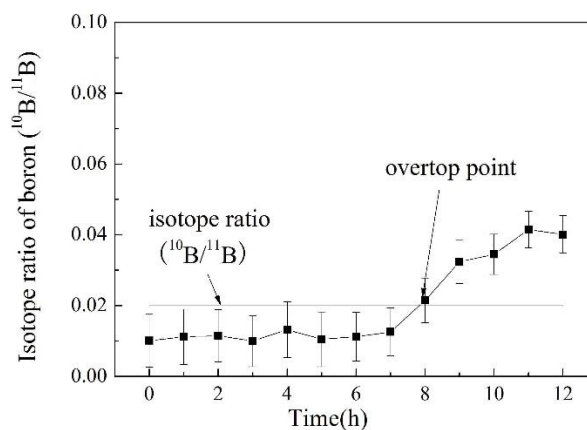
Figure 7. IR spectrograms of enriched BF_3 . (A) Spectrogram of an enriched $^{11}\text{BF}_3$ sample; (B) Spectrogram of an enriched $^{10}\text{BF}_3$ sample.

Table 5. Comparison of the results from the IR method and ICP-MS method.

Series No.	Isotope Ratio of $^{10}\text{B}/^{11}\text{B}$	
	Results of IR Method	Results of ICP-MS
1	1.6385 ± 0.0043	1.6390 ± 0.0006
2	0.7536 ± 0.0045	0.7546 ± 0.0010
3	0.4815 ± 0.0038	0.4832 ± 0.0009
4	0.0915 ± 0.0059	0.0905 ± 0.0010
5	0.0504 ± 0.0063	0.0488 ± 0.0012
6	0.0120 ± 0.0079	0.0102 ± 0.0007

3.5. Online Determination of Boron Isotope Ratio

Figure 8 illustrates the online determination results from the separation part of a chemical exchange rectification device, showing the enriched stage, the stability stage, and an instability point (where the isotope ratio suddenly drops). With the assistance of IR spectroscopy, the instability point can be found and thus encourage correction of the operation. Figure 9 shows the isotope ratio curve of the complex part where the $^{11}\text{BF}_3$ was enriched on the same isotope separation device. The errors of determination results were a little larger when the isotope ratio become smaller with the decrease in SNR. The sampling stage experiments lasted for 12 h and the sampling interval was 2 h. The curve shows the change of the isotope ratio in the process of product collection. The overtopping (exceeding limit value) point indicated that the sampling operation should be stopped at that moment, because the limit of the isotope ratio for ^{11}B product ($^{10}\text{B}/^{11}\text{B} \leq 0.0204$) has been exceeded.

**Figure 8.** Online determination results of the separation part of a chemical exchange rectification device.**Figure 9.** The curve of isotope ratio about the complex part of a chemical exchange rectification device.

4. Conclusions

A method was established to determine the isotope ratio of boron based on calculating the $2\nu_3$ region of BF_3 in infrared spectra used in a boron separation device to monitor the separation process online. The results showed that this has many benefits for a chemical exchange rectification device with the assistance of the online IR method. Response speed and measuring precision might be enhanced with further improvements such as the use fiber-optic technology.

Author Contributions: W.Z. and J.X. conceived and designed the experiments; Y.T. performed the experiments; Y.T. and J.X. analyzed the data; W.Z. contributed reagents/materials/analysis tools; Y.T. wrote the paper.

Funding: This research received no external funding.

Conflicts of Interest: The authors declare no conflicts of interest.

References

1. Zhang, L.; Zhang, W.J.; Xu, J.; Ren, X. Synthesis of enriched 10B boric acid of nuclear grade. *Trans. Tianjin Univ.* **2014**, *6*, 458–462. [[CrossRef](#)]
2. Zhang, W.J.; Liu, T.Y.; Xu, J. Preparation and characterization of 10B boric acid with high purity for nuclear industry. *Springerplus* **2016**, *1*, 1202–1212. [[CrossRef](#)] [[PubMed](#)]
3. Ferreira, T.H.; Miranda, M.C.; Rocha, Z.; Leal, A.S.; Comes, D.A.; Sousa, E.M.B. An Assessment of the Potential Use of BNNTs for Boron Neutron Capture Therapy. *Nanomaterials* **2017**, *4*, 82–92. [[CrossRef](#)] [[PubMed](#)]
4. Conn, A.L.; Wolf, J.E. Large-scale separation of boron isotopes. *Ind. Eng. Chem.* **1958**, *9*, 1231–1234. [[CrossRef](#)]
5. Sevryugova, N.N.; Uvarov, O.V.; Zhavoronkov, N.M. Determination of the separation coefficients of the isotopes of boron in the equilibrium evaporation of BCl_3 . *Sov. J. Atomic Energy* **1956**, *4*, 567–572. [[CrossRef](#)]
6. Zhang, L.; Zhang, W.J.; Xu, J.; Li, B. Preparation of boric-10 acid applied in nuclear industry. *Trans. Tianjin Univ.* **2015**, *2*, 172–177. [[CrossRef](#)]
7. Ivanov, V.A.; Katalnikov, S.G. Physico-Chemical and engineering principles of boron isotopes separation by using BF_3 -Anisole- BF_3 system. *Sep. Sci. Technol.* **2001**, *8–9*, 1737–1768. [[CrossRef](#)]
8. Yoneda, Y.; Uchijima, T.; Makishima, S. Separation of boron isotopes by ion exchange. *J. Phys. Chem.* **1959**, *12*, 2057–2058. [[CrossRef](#)]
9. Oi, T.; Tsukamoto, T.; Akai, H.; Kakihana, H.; Hosoe, M. Boron isotope separation by ion-exchange chromatography using an anion-exchange resin in halide forms: Separation factors at 25 °C. *J. Chromatogr. A* **1988**, *3*, 343–352. [[CrossRef](#)]
10. Rockwood, S.; Rabideau, S. Boron isotope separation by laser-induced photochemistry. *IEEE J. Quantum Electron.* **1974**, *9*, 789–790. [[CrossRef](#)]
11. Lyman, J.L.; Rockwood, S.D. Enrichment of boron, carbon, and silicon isotopes by multiple-photon absorption of $10.6\text{-}\mu\text{m}$ laser radiation. *J. Appl. Phys.* **1976**, *2*, 595–601. [[CrossRef](#)]
12. Wei, F.; Zhang, W.J.; Han, M.; Han, L.G.; Zhang, X.M.; Zhang, S.F. Operational policy of the boron isotopes separation by chemical exchange reaction and distillation. *Chem. Eng. Process.* **2008**, *1*, 17–21. [[CrossRef](#)]
13. Katalnikov, S.G.; Paramonov, P.M.; Nedzvetskii, V.S. Separation of boron isotopes using isotopic exchange between BF_3 and a complex of BF_3 with phenetole. *Sov. J. Atomic Energy* **1967**, *4*, 372–377. [[CrossRef](#)]
14. Lecuyer, C.; Grandjean, P.; Reynard, B.; Albarede, C.; Telouk, P. 11B/10B analysis of geological materials by ICP-MS Plasma 54: Application to the boron fractionation between brachiopod calcite and seawater. *Chem. Geol.* **2002**, *1*, 45–55. [[CrossRef](#)]
15. Porteous, N.C.; Walsh, J.N.; Jarvis, K.E. Measurement of boron isotope ratios in groundwater studies. *Analyst* **1995**, *5*, 1397–1400. [[CrossRef](#)]
16. Hepburn, C.A.; Vale, P.; Brown, A.S.; Simms, N.J.; McAdam, E.J. Development of on-line FTIR spectroscopy for siloxane detection in biogas to enhance carbon contactor management. *Talanta* **2015**, *141*, 128–136. [[CrossRef](#)] [[PubMed](#)]
17. Herrebout, W.A.; Lundell, J.; Van der Veken, B.J. Van der Waals complexes between unsaturated hydrocarbons and boron trifluoride: An infrared and ab initio study of ethyne BF_3 , propyne BF_3 and propyne $(\text{BF}_3)_2$. *J. Mol. Struct.* **1999**, *480*, 489–493. [[CrossRef](#)]

18. Herrebout, W.A.; Van der Veken, B.J. Vibrational spectra and relative stabilities of the van der Waals complexes of boron trifluoride with cis-2-butene, trans-2-butene and 2-methyl propene. *J. Mol. Struct.* **2000**, *550*, 389–398. [[CrossRef](#)]
19. Rayón, V.M.; Sordo, J.A. Van der Waals complexes between boron trifluoride and carbon monoxide: A theoretical study. *J. Phys. Chem. A* **1997**, *40*, 7414–7419. [[CrossRef](#)]



© 2018 by the authors. Licensee MDPI, Basel, Switzerland. This article is an open access article distributed under the terms and conditions of the Creative Commons Attribution (CC BY) license (<http://creativecommons.org/licenses/by/4.0/>).